

# Contribution of Hydrogen Bonds to Equilibrium $\alpha\beta$ Transition of Resorcinol

Masaki Yoshino, Kazuhiro Takahashi, Youhei Okuda, Takashi Yoshizawa, Nobuaki Fukushima, and Motosuke Naoki\*

Physical Chemistry Section, Bioscience Department, Faculty of Engineering, Gunma University, Kiryu, Gunma 376-8515, Japan

Received: July 23, 1998; In Final Form: February 2, 1999

The equilibrium  $\alpha\beta$  transition temperature,  $T_{\alpha\beta}$ , between the  $\alpha$  crystalline phase and the  $\beta$  crystalline phase of resorcinol has been determined when both supercooling and superheating effects vanished. The latent volume and  $dT_{\alpha\beta}/dP$  have been determined by use of a precision pycnometer, and the thermodynamic characteristics of the  $\alpha\beta$  transition are presented. The  $P$ – $V$ – $T$  relations of each phase have also been obtained. All of the thermal expansion coefficient, the isothermal compressibility, and the internal pressure for the higher-temperature, higher-density polymorph, the  $\beta$  crystal, are much larger than those for the lower-temperature, lower-density polymorph, the  $\alpha$  crystal. Contributions of the hydrogen bonds and the van der Waals energy to the internal energy have semiquantitatively been analyzed by use of a simple potential model. When the  $\alpha$  crystal transforms to the  $\beta$  crystal, the energy of hydrogen bonds decreases due to the breakdown of the hydrogen bonds, whereas the van der Waals energy increases with the contraction in volume. Since the latter cancels the most of the former, we observe the small latent heat. The breakdown of the hydrogen bonds induces a significant change in the potential depths of the covalent structure  $\text{O}-\text{H}\cdots\text{O}$  and ionic, proton-transferred structure  $\text{O}^-\cdots\text{H}-\text{O}^+$  in each hydrogen bond. In consequence, the distribution of the protons between the covalent structure and the ionic structure changes with the transition. The increase in the entropy produced from the redistribution of the protons is the same order of magnitude as the latent entropy.

## 1. Introduction

Resorcinol undergoes a phase transition, called the  $\alpha\beta$  transition, to a denser polymorph with an enthalpy increase at higher temperatures. The lower-temperature modification is called the  $\alpha$  crystal, and the higher-temperature one the  $\beta$  crystal.<sup>1</sup> Both crystals of resorcinol have lower density than the other dihydroxy benzenes.<sup>2</sup> Those structures were investigated with the X-ray diffraction by Robertson<sup>3</sup> and by Robertson and Ubbelohde.<sup>4</sup> More detailed structure of the  $\alpha$  crystal was determined with neutron diffraction by Bacon and Curry.<sup>5</sup> The  $\alpha$  crystal has an open structure maintained by the directive power of the hydrogen bonds, and the  $\beta$  crystal has a denser structure resembling molecular crystals.<sup>3–5</sup> The space group is the same for both crystals, belonging to the orthorhombic system of  $C_{2v}^9(Pna)$  with four molecules in the unit cell. In  $\alpha$ , all the angles of four C–O–O and two O–O–O except one C–O–O are fairly near the tetrahedral value of  $109.5^\circ$ ,<sup>3,5</sup> while all those angles in  $\beta$  are far from the tetrahedral value.<sup>4,6</sup> Bacon and Lisher<sup>6</sup> have found that the rigid-body thermal vibrations of the two phases are not drastically different and have suggested that the breakdown of the  $\alpha$  structure is attributable to the instability of the hydrogen bonds rather than to any direct effect of the thermal motion. In understanding the definite view on the nature of the  $\alpha\beta$  transition, problems are how the energy increment attended with the breakdown of the hydrogen bonds contributes to the latent heat, and what is the origin of the latent entropy. To solve these problems, exact thermodynamic characteristics of the transition, i.e., the equilibrium phase-transition temperature  $T_{\alpha\beta}$ , the latent volume  $\Delta V$ , the latent entropy  $\Delta S$ , and the latent enthalpy  $\Delta H$  are required.

Various values of  $T_{\alpha\beta}$  and of the latent quantities have been reported. Values of  $T_{\alpha\rightarrow\beta}$ , the transformation temperature from  $\alpha$  to  $\beta$ , in the literature range from 340 to 369 K.<sup>7</sup> Values of  $\Delta H$  in the literature range from 0.7 to 1.4 kJ mol<sup>-1</sup>.<sup>7–11</sup> In 1913, Lantz obtained  $T_{\alpha\rightarrow\beta}$  as 344 K and  $\Delta V$  as  $-2.63 \pm 0.36$  cm<sup>3</sup> mol<sup>-1</sup> from dilatometry.<sup>1</sup> This value of  $\Delta V$  has been used for calculations of the other transition characteristics by many authors. As we will show later, however, the usual dilatometry has been found not to be appropriate for determining the latent volume of this transition.

The equilibrium  $T_{\alpha\beta}$  should be the temperature when  $T_{\alpha\rightarrow\beta}$  coincides with  $T_{\beta\rightarrow\alpha}$ , the transformation temperature from  $\beta$  to  $\alpha$ . Little is known about,  $T_{\beta\rightarrow\alpha}$ . Lantz reported  $T_{\beta\rightarrow\alpha} > 328$  K from thermomechanic measurements.<sup>1</sup> Ban, Suga, and Seki showed that the  $\beta \rightarrow \alpha$  transformation was facilitated by adsorption of solvent vapor on the surface of the  $\beta$  crystal.<sup>8</sup> Deb et al observed that the  $\beta \rightarrow \alpha$  transformation took a long time at room temperature.<sup>12</sup> The difficulties in the determination of  $T_{\alpha\beta}$  are caused mainly by the slow transformation rates of both  $\alpha \rightarrow \beta$  and  $\beta \rightarrow \alpha$ , which, as a consequence, give rise to considerably large superheating and supercooling. The magnitude of superheating and supercooling depends also on rates of experimental scans, impurities, and existence of crystalline nuclei. To obtain reliable characteristics of the  $\alpha\beta$  transition, we have to overcome the experimental difficulties above.

At  $T_{\alpha\beta}$ , the Gibbs energy  $G$  of the two phases are identical, i.e.,  $\Delta G = \Delta H - T_{\alpha\beta}\Delta S = 0$ , and the Clausius–Clapeyron equation,  $dT_{\alpha\beta}/dP = \Delta V/\Delta S$ , holds. The positive  $\Delta H$  corresponds to the positive  $\Delta S$ , and the negative  $\Delta V$  corresponds to the negative  $dT_{\alpha\beta}/dP$ . In the present work, we have started to confirm the sign of  $dT_{\alpha\beta}/dP$  by DTA measurements.

\* Author to whom correspondence should be addressed.

Under atmospheric pressure, the enthalpy is almost equal to the internal energy  $E$ , i.e.,  $\Delta E \approx \Delta H$ . The internal energy increases with the breakdown of hydrogen bonds, but it decreases with the contraction in volume through the increase in the van der Waals (vdW) energy. Since the experimental  $\Delta H$  is positive, therefore, the decrease in the hydrogen-bond (HB) energy should overcome the increase in the vdW energy. Information on the internal energy can be obtained from the internal pressure,  $P_i$ , i.e., the slope of the average intermolecular potential energy,  $P_i \equiv (\partial E/\partial V)_T = T(\partial P/\partial T)_V - P$ , where the thermal-pressure coefficient,  $(\partial P/\partial T)_V$ , is available from the  $P$ - $V$ - $T$  relations of each phase.  $\Delta H$  caused from the increase in the vdW energy and the decrease in the HB energy corresponds to the difference in the entropy between two phases. A major source of the positive latent entropy should also be revealed.

This work consists (1) of the experiments determining the characteristics of the equilibrium transition: (1-1) the DTA measurements to outline the transition, (1-2) the repeated slow dilatometry to determine  $T_{\alpha\beta}$ , (1-3) the dilatometry under elevated pressures by use of a pressure pycnometer to determine the coexistence curve and  $\Delta V$ , (1-4) the  $P$ - $V$ - $T$  measurements to obtain  $P_i$ ; (2) of the analysis of the contributions to the internal energy by use of a simple potential model; and (3) of the analysis of the source of the latent entropy.

## 2. Experimental Section

**Sample.** Resorcinol was purchased from three companies, e.g., Mitsuwa Pure Chemicals Co., Wako Pure Chemical Ltd., and Aldrich Chemical Co., but there was no great difference among those samples. A repeated recrystallization from toluene solution was carried out to obtain the  $\alpha$  crystal. The solution grown sample with a needle shape (ca.  $1 \times 1 \times 30$  mm) was used for the density measurements by the floating method in  $n$ -hexane/ $\text{CCl}_4$  solution and for the dilatometry to get the thermal dilation of  $\alpha$  under atmospheric pressure. The result of the density measurements, unfortunately, was not employed in the final data as shown in the next section.

The sample was also purified by repeated zone-melting. The sample was inserted in a glass tube of 30 cm length, which was sealed in a vacuum. The glass tube was moved through the zone-melting equipment (four steps) at a rate of 12 h per run. After seven runs (28 steps), the glass tube was broken and the sample (transparent and colorless aggregate of 3–7 mm cubic single crystals) was taken out.

**DTA Measurements.** To outline the  $\alpha\beta$  transition, we tried a differential thermal analysis (DTA) under elevated pressures before the other experiments. As the latent heat was small, it was not easy to observe the reproducible  $\alpha \rightarrow \beta$  transformation by our equipment. We carried out the DTA measurements in the following manner. After the temperature had been increased to 370 K, the temperature was lowered and was kept at room temperature for 12 h. Since the  $\beta \rightarrow \alpha$  transformation did not become complete for 12 h at room temperature, some nucleus of the  $\beta$  form would remain in  $\alpha$ . At the next isobaric heating scan from the room temperature to 370 K at a rate of  $3.3 \text{ K min}^{-1}$ , the superheating was small due to contamination of the  $\beta$  nucleus, and we could observe the  $\alpha \rightarrow \beta$  transformation temperature reproducible within  $\pm 2$  K. The pressure was changed from 0.1 to 100 MPa by about 5 MPa intervals. The transmitting medium was Silicone oil (KF-96-30CS, Shin-Etsu Chemical Co.).

**Dilatometry under Atmospheric Pressure.** The volume–temperature ( $V$ - $T$ ) relations under atmospheric pressure were

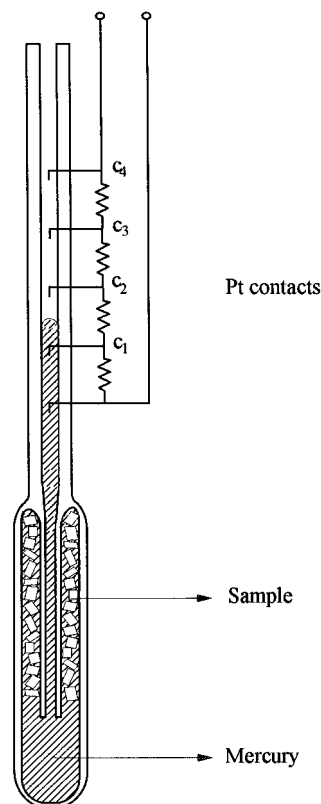


**Figure 1.** The pressure pycnometer.

obtained by the usual mercury-capillary dilatometry. Seven dilatometers were employed, e.g., three were to determine the thermal dilations,  $(\partial V/\partial T)_P$ , and four were to observe the hysteresis of the  $\alpha \rightarrow \beta$  and  $\beta \rightarrow \alpha$  transformations and to determine  $T_{\alpha\beta}$  and  $T_{\beta\alpha}$  at various scan rates. A large hysteresis in volume as well as in  $T_{\alpha\beta}$  was observed.

The thermal dilation of  $\alpha$  was obtained in the temperature range 245–340 K at a heating rate of  $0.33 \text{ K min}^{-1}$ . For  $\beta$ , the dilatometer was heated to 372 K (the  $\beta$  region) at a heating rate of  $0.143 \text{ K min}^{-1}$ . The volume started to decrease above 337.0 K (started to transform from  $\alpha$  to  $\beta$ ) and dropped rapidly above 358 K. We observed the sample shrink by about 16% of the latent volume during an annealing treatment at  $372 \pm 0.5$  K for 2 days. After the annealing, the sample was cooled to 350 K and heated to 382 K at a rate of  $0.33 \text{ K min}^{-1}$ . We observed no hysteresis in volume in the latter cooling and heating processes and obtained the thermal dilation of  $\beta$ .

**T-P Relations.** A pressure pycnometer designed for measuring the latent volume and the  $P$ - $V$ - $T$  relations is shown in Figure 1. When mercury touched one of the upper Pt wires ( $c_2$ – $c_4$ ), a change in the electric current (about 0.1 mA) could be detected from the outside of the pressure vessel. The apparent  $T$ - $P$  relations were measured in the following manner. When the electric circuit was open (for example, the top of the mercury column was between  $c_1$  and  $c_2$ ), the temperature was raised to  $T_1$  for the mercury to touch  $c_2$ . Then the pressure was slightly increased until the circuit came open (the top of the mercury column dropped below  $c_2$ ). Keeping  $T_1$ , we reduced the pressure slowly (ca.  $-0.1 \text{ MPa min}^{-1}$ ) until the mercury touched  $c_2$  again, and read the pressure  $P_1$  just when the mercury touched  $c_2$ . This series of the procedure was repeated, and  $T$ - $P$  relations of the same Pt wire (at the constant apparent volume of the pycnometer) were obtained. The experiments were carried out at about 2 K intervals from 258 to 388 K under 0.1 to 98 MPa. Silicone oil (KF-96-30CS, Shin-Etsu Chemical Co.) was used to

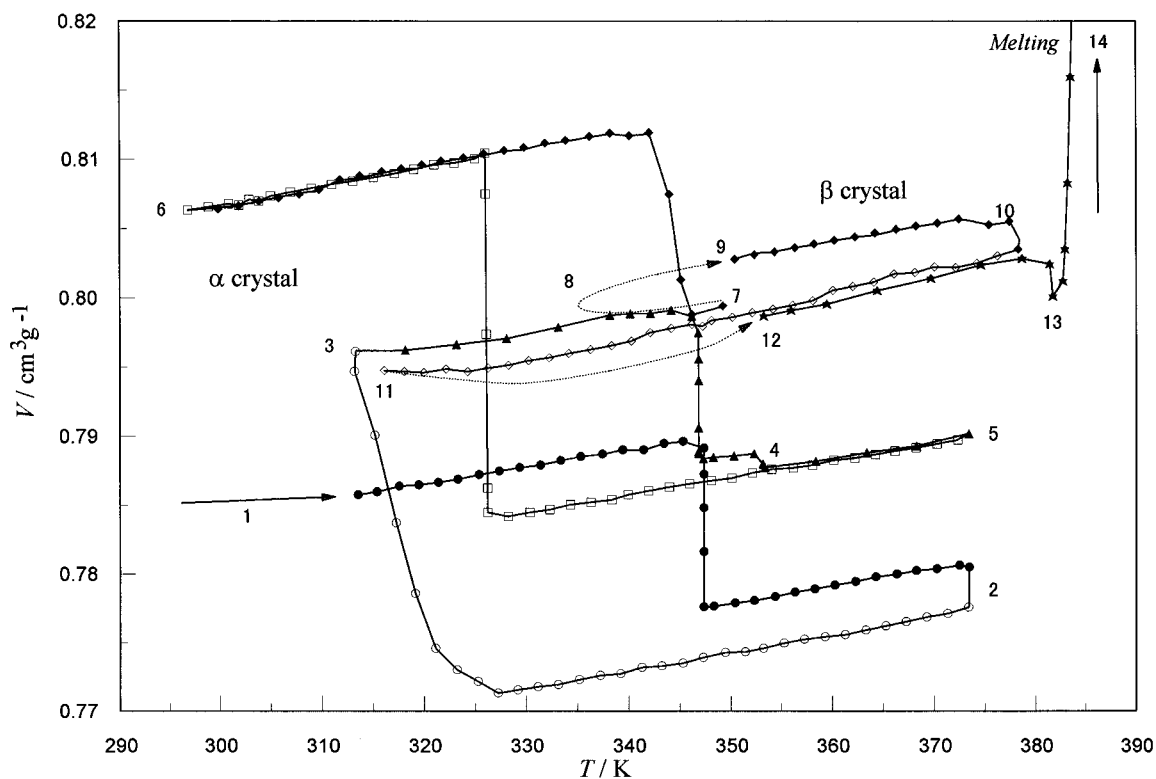


**Figure 2.** An example of the hysteresis of the dilatometry at 0.1 MPa. Closed symbols are heating scans, and open symbols are cooling scans. Plots 1→2, heated at a rate of  $0.146 \text{ K min}^{-1}$ ; 2, kept for 4 h; 2→3, cooled at a rate of  $-0.134 \text{ K min}^{-1}$ ; 3, kept for 3 h; 3→4, heated at a rate of  $0.085 \text{ K min}^{-1}$ ; 4, kept for 9 h; 4→5, heated at a rate of  $0.085 \text{ K min}^{-1}$ ; 5, kept for 2 h; 5→6, cooled at a rate of  $-0.097 \text{ K min}^{-1}$ , kept at 327 K for 1 day, and cooled to 297 K; 6, kept for 1 day; 6→7, heated at a rate of  $0.067 \text{ K min}^{-1}$ ; 7→8→9, cooled to 335 K, kept for 1 day, and heated to 350 K; 9→10, heated to 376 K at a rate of  $0.067 \text{ K min}^{-1}$ ; 10, kept for 6 h; 10→11, cooled at a rate of  $-0.163 \text{ K min}^{-1}$ ; 11→12→13→14, heated to the liquid at a rate of  $0.02 \text{ K min}^{-1}$ .

transmit the hydrostatic pressure. The pressure was measured by a Heise bourdon gauge with an automatic compensator (Dresser Ind.) within  $\pm 0.1 \text{ MPa}$ , and the temperature by a calibrated alumel–chromel thermocouple inserted in the pressure vessel within  $\pm 0.05 \text{ K}$ .

**DSC Measurements.** The transformation temperatures were also measured by a differential scanning calorimeter (Model DSC-9000, Shinku-Riko Co.) for seven different masses of the sample at the heating rates of 1, 3, 10,  $-1$ ,  $-3$ ,  $-7 \text{ K min}^{-1}$  through the temperature range of 253–373 K. We measured the latent heat also, but we did not employ the results on the latent heat in the final data as shown in the next section.

## Results

### Determination of the Equilibrium Transition Temperature.

Cyclic measurements by four dilatometers under atmospheric pressure were carried out to obtain the equilibrium transition temperature  $T_{\alpha\beta}$ . An example of the hysteresis in the transition region is shown in Figure 2. The starting temperature of the  $\alpha \rightarrow \beta$  transformation,  $T_{\alpha\rightarrow\beta}$ , and that of  $T_{\beta\rightarrow\alpha}$  are listed in Table 1. It is suggested that  $T_{\alpha\beta}$  should be between 337.0 K (the lowest temperature of  $T_{\alpha\rightarrow\beta}$ ) and 330.2 K (the highest temperature of  $T_{\beta\rightarrow\alpha}$ ). The results of the present slow, cyclic experiments are summarized as follows. (i) It is difficult to determine  $T_{\alpha\beta}$  only from a single slow experiment. (ii) The  $\alpha \rightarrow \beta$  transformation starts above 337 K and pronounced changes in volume occur around 345 K, but the transformation does not go to completion even in the slowest experiment (at a heating rate of  $0.067 \text{ K min}^{-1}$ , about 15–20% of the volume decrement remained unchanged as seen in Figure 2). (iii) The  $\beta \rightarrow \alpha$  transformation starts below 330 K and pronounced changes in

**TABLE 1: Apparent  $T_{\alpha\rightarrow\beta}$  and  $T_{\beta\rightarrow\alpha}$  Transformation Temperatures**

heating rate ( $\text{K min}^{-1}$ )	$T_{\alpha\rightarrow\beta}$ (K)	cooling rate ( $\text{K min}^{-1}$ )	$T_{\beta\rightarrow\alpha}$ (K)
Present Work			
0.33	351.4, 350.5	−0.33	330.2
0.33	347.8, 347.4	−0.33	324.0
0.274	337.6		
0.178	338.2	−0.163	322.9
0.146	346.9	−0.134	326.7
0.143	337.0		
0.085	343.8	−0.097	328.7
0.067	338.5		
0.038	340.2		
Literature			
	< 348 <sup>a</sup>		> 328 <sup>a</sup>
	$366.8 \pm 1.4$ <sup>b</sup>		
0.625	$369 \pm 6$ <sup>c</sup>		

<sup>a</sup> From thermomechanics: Lautz, H. Z. *Phys. Chem.* **1913**, 84, 611.

<sup>b</sup> From DTA: Sabbah, R.; Buluku, E. N. L. E. *Can. J. Chem.* **1991**, 69, 481. <sup>c</sup> From DSC: Ebisuzaki, Y.; Askari, L. H.; Bryan, A. M.; Nicol, M. F. *J. Chem. Phys.* **1987**, 87, 6659.

volume occur below 326 K, but the transformation rate becomes very slow below 310 K. (iv) In every cyclic process, the apparent volume increment of  $\beta \rightarrow \alpha$  is almost twice as large as the apparent volume decrement of  $\alpha \rightarrow \beta$ . (v) Notwithstanding the hysteresis in volume and temperature, the thermal dilation,  $(\partial V / \partial T)_P$ , of each crystal is almost reproducible.

$T_{\alpha\rightarrow\beta}$  and  $T_{\beta\rightarrow\alpha}$  are plotted against the heating and cooling rate in Figure 3. The broken lines indicate the limits of the ranges of  $T_{\alpha\rightarrow\beta}$  and  $T_{\beta\rightarrow\alpha}$ . All of the temperatures from the DSC measurements and those in the literature,<sup>1,5,10</sup> which were obtained at faster heating and cooling rates, lie within these

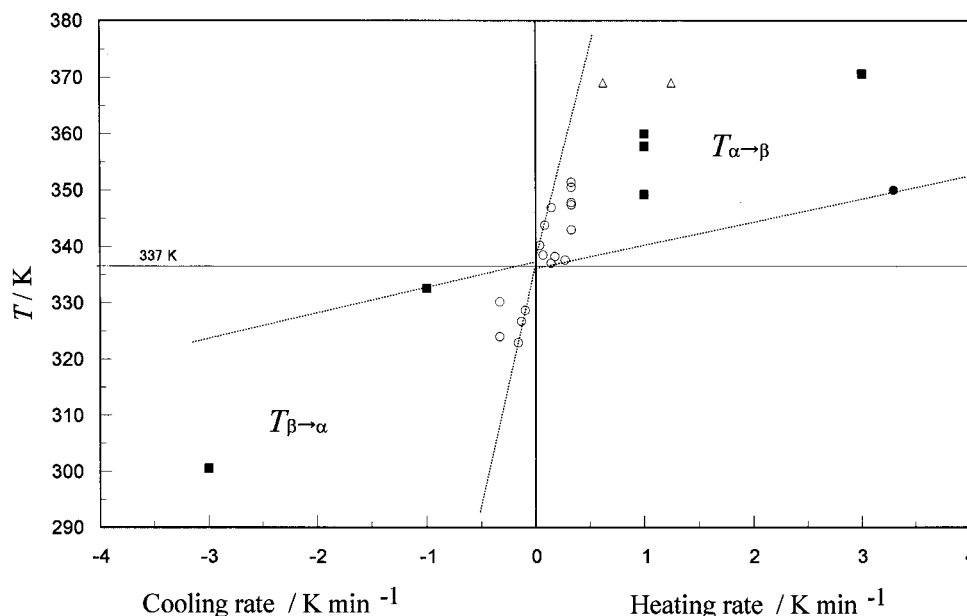


**Figure 3.** The  $\alpha \rightarrow \beta$  and  $\beta \rightarrow \alpha$  transformation-temperatures against heating and cooling rates. (○), dilatometry; (●), DTA; (■), DSC; (△), DSC by Ebisuzaki et al.<sup>7</sup> The dotted lines are upper and lower limits of the experiments.

limits. Both limits of  $T_{\alpha \rightarrow \beta}$  and  $T_{\beta \rightarrow \alpha}$  appear to become narrower as the experimental rates decrease. Extrapolating the limits to the zero heating and cooling rate, we have estimated  $T_{\alpha\beta}$  as  $337 \pm 1$  K.

The large volume hysteresis of the result (iv) was not observed under elevated pressures above 10 MPa. As shown in the later section, another volume hysteresis was observed below 2 MPa especially in the  $\alpha$  region, but almost disappeared above 3 MPa. When we observed the transformation from  $\beta$  to  $\alpha$  in a test tube, the transition started from the surface, many cracks grew in a few hours, and the test tube was broken after several days. It is suggested that the large volume hysteresis of (iv) probably arose from many small cracks that mercury could not invade, and that, when the pressure exceeded the surface tension of mercury, the hysteresis would disappear.

There have been some arguments that impurities in the sample may also affect  $T_{\alpha \rightarrow \beta}$  and  $T_{\beta \rightarrow \alpha}$ . Ebisuzaki et al. attended impurities and contended that  $T_{\alpha\beta} = 369 \pm 6$  K from the DSC measurements at heating rates of 0.625 and 1.25 K min<sup>-1</sup>.<sup>7</sup> The melting temperature drops considerably with impurities because of the significant decrease in the Gibbs energy of the liquid. In the present case (the crystal–crystal transition), however, effects of impurities on the transition may be more delicate when the impurities are not incorporated in the lattice of the crystals. As discussed by Ban et al.,<sup>8</sup> a small amount of impurities adsorbed on the surface of the crystals becomes rather an advantage to approach the equilibrium transition by reducing the superheating and supercooling effects.

In the present DSC measurement, the highest  $T_{\alpha \rightarrow \beta}$  was 370.6 K at a heating rate of 3 K min<sup>-1</sup> and the lowest one was 349.2 K at a heating rate of 1 K min<sup>-1</sup>.  $T_{\alpha \rightarrow \beta}$  depended on the histories of each sample rather than on the heating rate, e.g.,  $T_{\alpha \rightarrow \beta}$  of the sample kept longer in the  $\alpha$  region was much higher. This may be due to contamination of the trace of  $\beta$ , reducing the superheating effect.  $T_{\beta \rightarrow \alpha}$  was also observed by the DSC for samples kept 0.5–1 h at 375 K, but the temperature was ambiguous due to difficulties in the calibration of the temperature of cooling scan in the DSC instrument.

**The V–T Relations and the Latent Volume.** The average specific volume of the 44 solution-grown samples of  $\alpha$  measured

by the floating method was  $0.7835 \pm 0.0023$  cm<sup>3</sup> g<sup>-1</sup> at 303 K ( $0.7820 \pm 0.0024$  cm<sup>3</sup> g<sup>-1</sup> at 290 K), which was compared with  $0.7867$  cm<sup>3</sup> g<sup>-1</sup> at 293 K from the floating method by Lutz,<sup>1</sup>  $0.782$  cm<sup>3</sup> g<sup>-1</sup> at the room temperature from the X-ray diffraction by Robertson,<sup>3</sup> and  $0.77654$  cm<sup>3</sup> g<sup>-1</sup> at the room temperature from the neutron diffraction by Bacon and Curry.<sup>5</sup> The present result was close to that by Robertson. The experimental deviation, however, was considerably larger by about 1 order of magnitude than those obtained usually by the floating method in our laboratory. This might partly be due to small cracks formed in  $\alpha$ , which caused the volume hysteresis in the dilatometric measurements. Therefore, we have abandoned the use of the density from the floating method and adapted the value  $0.77654$  cm<sup>3</sup> g<sup>-1</sup> by Bacon and Curry as the reference volume of the atmospheric V–T relation of  $\alpha$ . It should be noted that such an ambiguous reference volume has little effect on the characteristics of the  $\alpha\beta$  transition and the other thermodynamic quantities.

The V–T relation of  $\alpha$  under the atmospheric pressure is expressed by

$$V_{\alpha} = 0.74307 + 0.000114_2 \times T \quad (3.1)$$

where  $V_{\alpha}$  is in cm<sup>3</sup> g<sup>-1</sup> and  $T$  is in K. The difference in volume between  $\alpha$  and  $\beta$  has been determined from the T–P relations obtained by the pressure pycnometer in the following manner. As the latent volume of the  $\alpha\beta$  transition is negative, the volume dilation with temperature in each phase is canceled from the volume decrement at the transition. Consequently, the same Pt–mercury contact of the same pycnometer with the same mercury and sample appears over  $\alpha$  and  $\beta$  as shown in Figure 4. Every extrapolation of the T–P lines to 0.1 MPa for the same symbol in Figure 4 (the data below 2 MPa were not adapted because they deviated from the T–P lines due to the effect of the strong surface tension of mercury) gives a volume difference between  $\alpha$  and  $\beta$ . The volume of the pressure pycnometer at 299 K can be calculated as a sum of the mercury and the  $\alpha$  sample. As the temperature increases from 299 to 375 K, the volume of the pycnometer increases following the thermal dilation of the Pyrex glass. Then the volume of  $\beta$  at 375 K is given by subtracting the volume of mercury from the volume of the



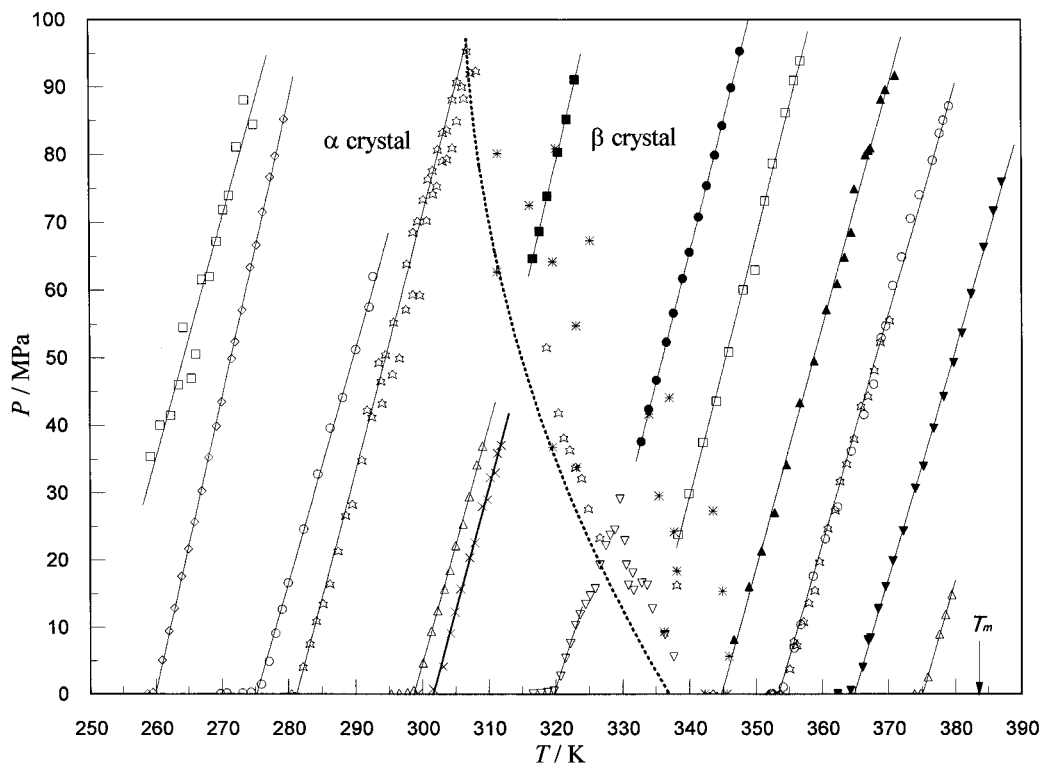


**Figure 4.**  $T$ - $P$  relations by the pressure pycnometers and  $T_{\alpha-\beta}$  from the preliminary DTA measurements(\*). The same symbols correspond to the same Pt-mercury contact of the pycnometer.  $\square$ ,  $\circ$ , and  $\triangle$  cover the whole  $\alpha$  and  $\beta$  regions. The dotted line is the estimated coexistence curve between  $\alpha$  and  $\beta$ . Thin solid lines are the linear fittings of the same Pt-mercury contact.

pycnometer at that temperature. Combining the results of the three Pt-mercury contacts with the results of the thermal dilation of  $\beta$ , we have

$$V_{\beta} = 0.70568 + 0.000146_{8} \times T \pm 0.00007 \quad (3.2)$$

where  $V_{\beta}$  and  $T$  are in  $\text{cm}^3 \text{g}^{-1}$  and K, respectively. The specific volume of  $\beta$  extrapolated to 293 K is  $0.74870 \text{ cm}^3 \text{g}^{-1}$ , which agrees with the value  $0.748 \text{ cm}^3 \text{g}^{-1}$  from the X-ray diffraction by Robertson and Ubbelohde.<sup>4</sup>

The latent volume is the volume difference between  $\alpha$  and  $\beta$  at  $T_{\alpha\beta}$  ( $= 337 \text{ K}$ ). The latent volume at  $337 \text{ K}$  under  $0.1 \text{ MPa}$  obtained from eqs 3.1 and 3.2 is  $-0.02640 \pm 0.00007 \text{ cm}^3 \text{g}^{-1}$ , which is larger by about 10% than that obtained by Lautz.<sup>1</sup> It should be emphasized that the experimental errors in  $\Delta V$  are free from the hysteresis in volume and may arise only from the sensitivity of contacts between mercury and Pt wire, and that the other errors (in the weights of the sample and mercury, and in the thermal expansion coefficients of mercury and Pyrex glass) are negligibly small in the present temperature range.

**The Latent Enthalpy and the Latent Entropy.** The  $dT_{\alpha-\beta}/dP$  obtained from the preliminary DTA experiments is  $-0.51 \pm 0.07 \text{ K MPa}^{-1}$  in the range of  $0.1$ – $90 \text{ MPa}$ . We tried a more accurate method to detect the coexistence curve by the pressure pycnometer. The temperature of the pycnometer was raised by about  $0.3$ – $0.5 \text{ K}$  step around the transition region. At each step, we kept the temperature for  $0.5$ – $1 \text{ h}$  and then reduced the pressure slowly (preventing any temperature drifts from an adiabatic expansion) and searched the pressure just when the mercury touched the Pt wire. The  $T_{\alpha-\beta}$ - $P$  data thus obtained are shown as stars and triangles along the dotted line in Figure 4. Since the experimental rate of this procedure was very slow, the slope,  $dT_{\alpha-\beta}/dP$ , would be expected to be close to the equilibrium coexistence curve between  $\alpha$  and  $\beta$ . The dotted curve drawn through  $T_{\alpha\beta}$  is the  $T_{\alpha\beta}$ - $P$  relation estimated from

**TABLE 2: Characteristics of the Equilibrium  $\alpha\beta$  Transition under Atmospheric Pressure**

		Present Work
$T_{\alpha\beta}$ , K		$337 \pm 1$
$\Delta V$ , $\text{cm}^3 \text{mol}^{-1}$		$-2.908 \pm 0.012$
$dT_{\alpha\beta}/dP$ , $\text{K MPa}^{-1}$		$-0.627 \pm 0.018$
$\Delta H$ , $\text{kJ mol}^{-1}$		$1.563 \pm 0.067$
$\Delta S$ , $\text{J K}^{-1} \text{mol}^{-1}$		$4.64 \pm 0.14$
		Literature
$\Delta V$ , $\text{cm}^3 \text{mol}^{-1}$		$-2.63 \pm 0.36^a$ at $344 \text{ K}$
$\Delta H$ , $\text{kJ mol}^{-1}$		$0.920 \pm 0.210^b$ heat of dissolution at $273 \text{ K}$
		$1.00^c$ DSC
		$1.210 \pm 0.080^d$ micro-calorimetry at $309 \text{ K}$
		$1.370 \pm 0.007^e$ DSC at $369 \text{ K}$
$\Delta S$ , $\text{J K}^{-1} \text{mol}^{-1}$		$3.71 \pm 0.05^e$ DSC at $369 \text{ K}$

<sup>a</sup> Lautz, H. Z. *Phys. Chem.* **1913**, *84*, 611. <sup>b</sup> Robertson, J. M.; Ubbelohde, A. R. *Proc. R. Soc. London* **1938**, *A167*, 136. <sup>c</sup> Suga, H.; Nakatsuka, K.; Shinoda, T.; Seki, S. *Nihonkagakuzasshi* **1961**, *82*, 29. <sup>d</sup> Ban, T.; Suga, H.; Seki, S. *Nihonkagakuzasshi* **1971**, *92*, 942. <sup>e</sup> Ebisuzaki, Y.; Askari, L. H.; Bryan, A. M.; Nicol, M. F. *J. Chem. Phys.* **1987**, *87*, 6659.

the  $dT_{\alpha-\beta}/dP$ .  $T_{\alpha\beta}$  appears to reach to around  $400 \text{ MPa}$  at room temperature, which agrees with  $T_{\alpha-\beta}$  observed from the X-ray diffraction by Sharma et al.<sup>13</sup> and from the Raman scattering by Ebisuzaki et al.<sup>7</sup> and Deb et al.<sup>12</sup>

The latent heat calculated from the Clausius-Clapeyron equation is  $1.563 \pm 0.067 \text{ kJ mol}^{-1}$  at  $337 \text{ K}$ , which is much higher than the literature value as seen in Table 2. As discussed in the earlier section, since the complete transformation requires more than several hours of annealing above  $370 \text{ K}$ , the low  $\Delta H$  from the calorimetry may be due to the incomplete  $\alpha \rightarrow \beta$  transformation.

Robertson and Ubbelohde reported  $\Delta H = 0.92 \pm 0.21 \text{ kJ mol}^{-1}$  at  $273 \text{ K}$  from the heat of dissolution.<sup>9</sup> Their experiment is independent of the transition rate and seems to be an

**TABLE 3: Parameters in the Polynomial,  $v = \sum_{i,j} c(i,j)T^iP^j$ , where  $v$ ,  $T$ , and  $P$  are in  $\text{cm}^3 \text{g}^{-1}$ , K, and MPa, respectively**

	$\alpha$ crystal		$\beta$ crystal	
	$c(0,j)$	$c(1,j)$	$c(0,j)$	$c(1,j)$
$c(i,0)$	0.743079	$1.1418 \times 10^{-4}$	0.705688	$1.4676 \times 10^{-4}$
$c(i,1)$	$-7.1606 \times 10^{-5}$	$-1.2062 \times 10^{-7}$	$-8.2092 \times 10^{-5}$	$-8.6806 \times 10^{-8}$
$c(i,2)$	$-2.7719 \times 10^{-7}$	$1.2159 \times 10^{-9}$	$2.2478 \times 10^{-7}$	$-3.3060 \times 10^{-10}$
$c(i,3)$	$2.3151 \times 10^{-9}$	$-4.5390 \times 10^{-12}$		
STD of $v$		0.000250		0.000152
region of $T/K$ (0.1 MPa)		260 ~ 320		345 ~ 375
region of $T/K$ (80 MPa)		270 ~ 300		322 ~ 386

**TABLE 4: Thermal-Pressure Coefficients as a Function of the Specific Volume,  $(\partial P/\partial T)_V = \sum_i c(i)v^i$ , in  $\text{MPa K}^{-1}$** 

	$\alpha$ crystal	$\beta$ crystal	$\alpha$ and $\beta$ crystal
$c(0)$	283678.114	140.2421	1446.0315
$c(1)$	-1098136.790	-354.3563	-5621.1166
$c(2)$	1417003.819	225.6873	7305.7669
$c(3)$	-609491.831		-3172.1789
STD	0.0075	0.00108	0.0018
region of $v/\text{cm}^3 \text{g}^{-1}$	0.767 ~ 0.777	0.745 ~ 0.759	0.745 ~ 0.777

appropriate method to determine the equilibrium  $\Delta H$ . Their result, however, is very small. As discussed in the earlier section, the  $\beta \rightarrow \alpha$  transformation rate is very slow below 310 K, but not above 310 K. Some contamination of  $\alpha$  might presumably exist in their  $\beta$  crystal.

The latent entropy is  $4.64 \pm 0.14 \text{ J K}^{-1} \text{ mol}^{-1}$  ( $= 0.558R$ ) at 337 K. This suggests that some degrees of freedom in the molecular configuration arise in the  $\beta$  crystal, which will be discussed in the later section.

**The  $P$ - $V$ - $T$  Relations.**  $P$ - $T$  relations at each Pt-mercury contact are shown in Figure 4. The volume of the sample at each pressure was calculated by subtracting the volume of mercury from the volume of the pycnometer. Specific-volume data were fitted to a polynomial for each phase. The parameters of each polynomial are listed in Table 3. The standard deviation (STD) of  $\alpha$  is larger than  $\beta$  because of the large experimental errors in the higher-pressure, lower-temperature region of  $\alpha$ . Since the transformation rate from  $\beta$  to  $\alpha$  is very slow in this region, some contamination of small fragments of  $\beta$  might impair the reproducibility of the data.

The thermal-pressure coefficients,  $(\partial P/\partial T)_V$ , obtained from slopes of the  $P$ - $T$  isochores, have been fitted to a polynomial as a function of volume. The parameters of the polynomial are listed in Table 4. The thermal-pressure coefficients of  $\beta$  and those of  $\alpha$  at the higher-volume region can be expressed by a single curve (the fourth column of Table 4).

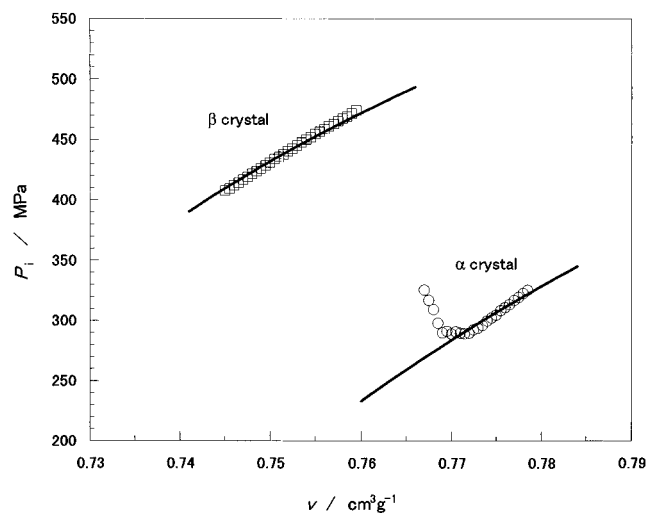
The thermal-expansion coefficients,  $(\partial \ln V/\partial T)_P$ , the isothermal compressibilities,  $-(\partial \ln V/\partial P)_T$ , and  $(\partial P/\partial T)_V$  at the  $\alpha\beta$  transition are compared in Table 5. The uncertainty in the derivatives estimated from the consistency among  $-(\partial \ln V/\partial P)_T$ ,  $(\partial \ln V/\partial T)_P$ , and  $(\partial P/\partial T)_V$  is about 5~8% for  $\alpha$  and about 0.8% for  $\beta$ . All of  $-(\partial \ln V/\partial P)_T$ ,  $(\partial \ln V/\partial T)_P$ , and  $(\partial P/\partial T)_V$  for the higher-density phase ( $\beta$ ) are significantly larger than those of the lower-density phase ( $\alpha$ ).

The internal pressures  $P_i$  are plotted in Figure 5. The data in the lower-volume region (in the lower-temperature and higher-pressure region) of  $\alpha$  are scattered.  $P_i$  of  $\beta$  is about 1.5 times larger than that of  $\alpha$ . This implies that the slope of the average potential of  $\beta$  against volume is much steeper than that of  $\alpha$ . We have had here information on the potentials of the two phases, i.e., its slopes and the difference at the transition (the latent enthalpy). In the next section, we will try to analyze the contributions of the hydrogen bonds to the internal energy.

**TABLE 5: Thermodynamic Properties at the  $\alpha\beta$  Transition**

$P$ , MPa	0.1	50
$T_{\alpha\beta}$ , K	$337 \pm 1$	$315 \pm 2$
$V_{\alpha}$ , $\text{cm}^3 \text{g}^{-1}$	$0.78155^a$	$0.77394 \pm 0.00025$
$V_{\beta}$ , $\text{cm}^3 \text{g}^{-1}$	$0.75515 \pm 0.00007$	$0.74675 \pm 0.00015$
$(\partial \ln V/\partial T)_P^{\alpha} \times 10^4$ , $\text{K}^{-1}$	$1.46 \pm 0.02$	$1.43 \pm 0.06$
$(\partial \ln V/\partial T)_P^{\beta} \times 10^4$ , $\text{K}^{-1}$	$1.94 \pm 0.02$	$1.89 \pm 0.02$
$-(\partial \ln V/\partial P)_T^{\alpha} \times 10^4$ , $\text{MPa}^{-1}$	$1.44 \pm 0.02$	$1.19 \pm 0.07$
$-(\partial \ln V/\partial P)_T^{\beta} \times 10^4$ , $\text{MPa}^{-1}$	$1.47 \pm 0.02$	$1.30 \pm 0.02$
$(\partial P/\partial T)_V^{\alpha}$ , $\text{MPa K}^{-1}$	$1.003 \pm 0.017$	$1.106 \pm 0.045$
$(\partial P/\partial T)_V^{\beta}$ , $\text{MPa K}^{-1}$	$1.394 \pm 0.002$	$1.477 \pm 0.002$

<sup>a</sup> Based on the lattice constant from the neutron diffraction by Bacon and Curry.<sup>5</sup>

**Figure 5.** The internal pressure as a function of the specific volume. Lines are the theory, eq 4.4.

#### 4. Analysis of the Configurational Energy by Use of Simple Potentials

The  $P$ - $T$  isochores of  $\beta$  are exactly linear. Thus, we regard the internal energy as a simple sum of a volume-independent term and a volume-dependent term. The  $P$ - $T$  isochores of  $\alpha$  are slightly convex upward, but the standard deviation of the linear fittings is below the experimental errors. We assume for both  $\alpha$  and  $\beta$  that

$$E^j = E_c^j(T, V) + E_k^j(T) \quad (4.1)$$

where the subscripts  $c$  and  $k$  denote the configurational term and the kinetic term, respectively, and the superscript  $j$  denotes the phase of  $\alpha$  or  $\beta$ . As the thermal molecular motions may not be significantly different between  $\alpha$  and  $\beta$  from the results of the neutron-diffraction study by Bacon and Lisher,<sup>6</sup> we assume

that  $E_c^\alpha \approx E_c^\beta$ . Then the difference in the configurational energy is equal to the difference in the internal energy, which is equal to the latent enthalpy under the atmospheric pressure, i.e.,  $E_c^\beta - E_c^\alpha \approx E^\beta - E^\alpha \approx \Delta H$ .

Assuming the configurational energy of the hydrogen-bonded crystal to consist of the HB energy and the vdW energy whose contribution may be described by the Lennard-Jones (LJ) potential,<sup>14,15</sup> we have employed the following expression for the total configurational energy:

$$E_c^j = E_{LJ}^j + E_{HB}^j = E^*[(1 - g^j x)(y^4 - 2y^2) + e^j x(y^4 - my)] \quad (4.2)$$

where

$$y = V^*/V, E^* = (1/2)Nz\epsilon_{LJ}, e^j = \epsilon_{HB}^j/\epsilon_{LJ}, x = N_{HB}/Nz \quad (4.3)$$

$y$  is the reduced density and  $V^*$  and  $V$  are the molar vdW volume of the molecule and the molar volume of the crystal, respectively.  $\epsilon_{LJ}$  and  $\epsilon_{HB}^j$  are the energy constants of the LJ potential and the HB potential of the  $j$  phase, respectively.  $N$  and  $N_{HB}$  are the Avogadro number and the number of groups forming the hydrogen bonds, respectively.  $z$  is the coordination number per molecule and  $g^j$  is the geometrical parameter which corrects an excluded volume effect of each hydrogen bond in the  $j$  phase.  $m$  is the parameter to adjust the balance between the repulsive and attractive contributions in the HB energy. Details of the derivation of eq 4.2 are given in the Supporting Information.

We have adopted the vdW volume of resorcinol as  $V^* = 61.92 \text{ cm}^3 \text{ mol}^{-1}$  obtained by Bondi's method<sup>17</sup> and the fraction of the HB contacts as  $x = 4/z$ , and have assumed that  $\epsilon_{LJ}$  of  $\alpha$  is the same as that of  $\beta$ . That is, all of  $V^*$ ,  $E^*$ ,  $\epsilon_{LJ}$ ,  $x$ ,  $z$ , and  $m$  are common to  $\alpha$  and  $\beta$ . Only  $\epsilon_{HB}^j$  and  $g^j$  are the parameters characterizing each crystal.

The internal pressure is expressed by

$$P_i^j = -(E^*/V^*)[4(1 - g^j x)(y^5 - y^3) + e^j x(4y^5 - my^2)] \quad (4.4)$$

When the theoretical  $\log[-4(1 - g^j x)(y^5 - y^3) - e^j x(4y^5 - my^2)]$  for  $\alpha$  and  $\beta$  against  $y$  are simultaneously superposed to the experimental  $\log P_i^j$ , the magnitude of the shift of the superposition gives  $\log(E^*/V^*)$ . We have fixed the value of  $m$  as 1.125 in the present calculation, because the HB term in eq 4.2, i.e.,  $(y^4 - my)$ , with  $m = 1.125$  for ice Ih has a minimum around 0 K. Values of the five unknown parameters,  $\epsilon_{LJ}$  or  $z$ , and  $\epsilon_{HB}^\alpha$ ,  $\epsilon_{HB}^\beta$ ,  $g^\alpha$ , and  $g^\beta$  have been determined by adjusting the theory to the five experimental facts,  $P_i^\alpha$  and  $P_i^\beta$ , their volume dependencies, and  $E_c^\beta - E_c^\alpha \approx \Delta H$ . Resulting values of the parameters are listed in Table 6S in Supporting Information. The theory appears to reproduce the experimental internal pressures and their volume dependencies well, except the higher-density region of  $\alpha$ , as shown in Figure 5.

The potential curves are shown in Figure 6, and the contributions to the configurational energy at  $T_{\alpha\beta}$  are listed in Table 7S. The HB potential is major in  $\alpha$ , while the LJ potential is major in  $\beta$ . The breakdown of the hydrogen bonds of  $\alpha$  creates  $12.83 \text{ kJ mol}^{-1}$  energy, but  $11.27 \text{ kJ mol}^{-1}$  decrease in the LJ energy cancels, and the increment of the total energy (the latent enthalpy) observed experimentally is only  $1.56 \text{ kJ mol}^{-1}$ . The larger internal pressure of  $\beta$  rather than  $\alpha$  in Figure 5 arises from the steeper slope of the LJ potential rather than HB potential. The difference in the LJ energy between  $\alpha$  and  $\beta$  arises partly from the larger density of  $\beta$  than  $\alpha$  and partly from the fact that the excluded-volume effect of hydrogen bonds in  $\alpha$  is

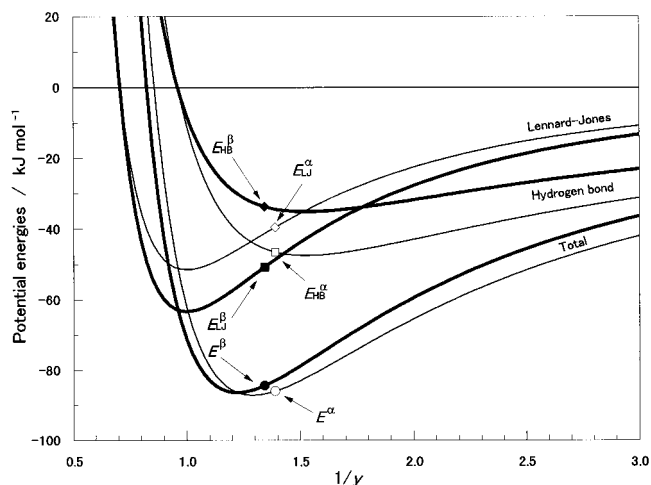


**Figure 6.** Contributions of the Lennard-Jones energy and the hydrogen-bond energy to the configurational energy as a function of the reduced volume. Thin lines and open symbols are for the  $\alpha$  crystal and thick lines and closed symbols are for the  $\beta$  crystal. Arrows indicate the contributions at  $T_{\alpha\beta}$ .

stronger than  $\beta$ . The linear O—H···O bonds in  $\alpha$  rather than the bending O—H···O bonds in  $\beta$  may hinder adjacent molecular contacts.

The average HB energy per one hydrogen bond is  $23.23 \text{ kJ mol}^{-1}$  ( $5.55 \text{ kcal mol}^{-1}$ ) in  $\alpha$  and  $16.81 \text{ kJ mol}^{-1}$  ( $4.02 \text{ kcal mol}^{-1}$ ) in  $\beta$ . Though the hydrogen bonds in  $\alpha$  may be almost perfect, the HB energy in  $\beta$  is small, as is the LJ energy. In the energetic point of view, the formation of hydrogen bonds seems not to be inevitable in  $\beta$ . An entropic demand to reduce the free energy of  $\beta$ , as discussed in the next section, may play an important role for the formation of the weak hydrogen bonds in  $\beta$ .

In the present investigation, we tried several functional forms for the HB energy in eq 4.2, e.g.,  $(y^4 - my^{1/3})$ ,  $(y^4 - my^{2/3})$ ,  $(y^5 - my)$ , etc. The resulting values of  $E_{LJ}^j$  and  $E_{HB}^j$  were not qualitatively different from the present results, i.e.,  $E_{LJ}^\beta - E_{LJ}^\alpha = -9 \sim -12 \text{ kJ mol}^{-1}$  and  $E_{HB}^\beta - E_{HB}^\alpha = 10 \sim 13 \text{ kJ mol}^{-1}$ . The functional form of the HB energy did not affect the essential result.

## 5. Redistribution of Protons between Covalent and Ionic Structures of Hydrogen Bonds

As the difference in the Gibbs energy between two phases disappears at the equilibrium phase transition, the latent enthalpy is completely compensated by the increase in the entropy (the latent entropy). Following the result by Bacon and Lisher that the rigid-body thermal vibrations of the two phases are not drastically different, most of the increase in the entropy should be an increase in the configurational entropy. We will demonstrate a possibility of the source of the entropy increase that is associated with the weak hydrogen bonds in  $\beta$ .

A hydrogen bond has the covalent structure and ionic structure. The breakdown of the hydrogen bonds may mainly correspond to the breakdown of the covalent structures, because the bending of O—H···O in  $\beta$  may scarcely influence the isotropic ionic potential. According to cross sections of the Lippincott—Schroeder potential,<sup>18</sup> the HB potential exhibits two minima when plotted as a function of O—H distance. The inner minimum corresponds to the covalent structure, O—H···O and the outer minimum corresponds to the ionic, proton-transferred structure, O<sup>-</sup>···H—O<sup>+</sup>. In the equilibrium, the hydrogen atoms are distributed in these two minima. From the neutron diffraction

on  $\alpha$  by Bacon and Curry,<sup>5</sup> the hydrogen atom locates near the oxygen atom (the O–H distance is 1.02 Å), and the covalent minimum may be much deeper than the ionic minimum in  $\alpha$ . Considering only the ground state of each hydrogen bond, we can simply write the partition function  $Z$  for the two minima of each hydrogen bond:

$$Z = \exp(-\epsilon_{\text{cov}}^j/kT) + \exp(-\epsilon_{\text{ion}}^j/kT) \quad (5.1)$$

where  $\epsilon_{\text{cov}}^j$  and  $\epsilon_{\text{ion}}^j$  are the minimum energies of the covalent structure and the ionic structure, respectively, and  $k$  is the Boltzmann constant. The boundary conditions are

$$E_{\text{HB}}^j = N_{\text{cov}}^j \epsilon_{\text{cov}}^j + N_{\text{ion}}^j \epsilon_{\text{ion}}^j \quad (5.2)$$

$$2N = N_{\text{cov}}^j + N_{\text{ion}}^j \quad (5.3)$$

From eqs 5.1–5.3 and the Helmholtz energy,  $A = -kT \ln Z$ , we have the following simple relation.

$$E_{\text{cov}}^j - E_{\text{ion}}^j = RT \ln[(2E_{\text{cov}}^j - E_{\text{HB}}^j)/(E_{\text{HB}}^j - 2E_{\text{ion}}^j)] \quad (5.4)$$

where  $R$  is the gas constant, and  $E_{\text{cov}}^j = N\epsilon_{\text{cov}}^j$  and  $E_{\text{ion}}^j = N\epsilon_{\text{ion}}^j$ . Equation 5.4 includes two unknown energies,  $E_{\text{cov}}^j$  and  $E_{\text{ion}}^j$ , for each phase. When one of them is given, the other can be solved and the distribution of protons can be determined.

The difference in the distribution of protons between the two phases is expressed by the entropy difference obtained from eq 5.1:

$$S_{\text{HB}}^\beta - S_{\text{HB}}^\alpha = 2R(\chi_{\text{cov}}^\alpha \ln \chi_{\text{cov}}^\alpha + \chi_{\text{ion}}^\alpha \ln \chi_{\text{ion}}^\alpha - \chi_{\text{cov}}^\beta \ln \chi_{\text{cov}}^\beta - \chi_{\text{ion}}^\beta \ln \chi_{\text{ion}}^\beta) \quad (5.5)$$

where  $\chi_{\text{cov}}^j$  and  $\chi_{\text{ion}}^j$  are the fractions of the covalent structure and the ionic structure, respectively, defined by  $\chi_{\text{cov}}^j = N_{\text{cov}}^j/2N$ ,  $\chi_{\text{ion}}^j = N_{\text{ion}}^j/2N$ , and  $\chi_{\text{cov}}^j + \chi_{\text{ion}}^j = 1$ .

It is found from eqs 5.4 and 5.5 that the value of  $E_{\text{ion}}^\beta$  to give  $S_{\text{HB}}^\beta - S_{\text{HB}}^\alpha = 0.558R$  is around  $-11 \sim -12$  kJ mol<sup>-1</sup>. As the ionic potential is isotropic,  $E_{\text{ion}}^\alpha$  may not much differ from  $E_{\text{ion}}^\beta$ . Distributions of protons of the hydrogen bonds for  $S_{\text{HB}}^\beta - S_{\text{HB}}^\alpha = 0.558R$  and  $E_{\text{ion}}^\alpha \approx E_{\text{ion}}^\beta = -11.79$  kJ mol<sup>-1</sup> have been calculated as  $\chi_{\text{ion}}^\alpha = 1.55\%$ ,  $\chi_{\text{ion}}^\beta = 11.62\%$ ,  $\chi_{\text{cov}}^\alpha = 98.45\%$ , and  $\chi_{\text{cov}}^\beta = 88.38\%$ . In this case, more than 98% of the protons of  $\alpha$  lie in the covalent well, and  $E_{\text{cov}}^\alpha$  is almost equal to the HB energy. On the other hand, about 12% of the protons of  $\beta$  lie in the ionic well, and  $E_{\text{cov}}^\beta$  is slightly larger than the HB energy. It may be interesting that only 12% redistribution of the protons of the hydrogen bonds produces the increment of  $0.558R$  in the entropy. We do not claim that the  $S_{\text{HB}}^\beta - S_{\text{HB}}^\alpha$  from the present investigation is exactly equal to the latent entropy. It should be emphasized that the breakdown of the hydrogen bonds induces the redistribution of protons in the hydrogen bonds and produces an entropy increment similar in magnitude to the latent entropy, which reduces the free energy and stabilizes the weak hydrogen bonds in  $\beta$ .

## 6. Summary and Conclusions

The  $\alpha\beta$  transition accompanies a decrement in volume. Generally both the enthalpy and the entropy decrease as the volume decreases, whereas the latent enthalpy and the latent entropy of this phase transition is positive. A key for solving this peculiarity has been given from the X-ray and the neutron diffraction studies by Robertson,<sup>2</sup> Robertson and Ubbelohde,<sup>3</sup> Bacon and Curry,<sup>4</sup> and Bacon and Lisher.<sup>5</sup> They suggested the

breakdown of the hydrogen bonds in the  $\alpha$  crystal. It remains why the entropy increment occurs with the volume decrement.

The quantitative analysis requires exact values of the latent enthalpy and the latent entropy, which can be determined at the equilibrium transition. In the present work, therefore, the determination of the equilibrium transition temperature was the first problem. Since both  $\alpha \rightarrow \beta$  and  $\beta \rightarrow \alpha$  transformation rates were very slow, superheating and supercooling could not be avoided in the finite experimental rates. We have carried out many slow experiments and have determined the equilibrium transition temperature as the temperature when the effects of superheating and supercooling would vanish.

The  $P$ – $V$ – $T$  relations offer information on the potential energy curve through the internal pressure. The internal pressure of  $\beta$  is much higher than that of  $\alpha$ . This suggests that the potential curves of  $\alpha$  and  $\beta$  differ significantly from each other. The internal energy of each phase was expressed by the combination of two simple potentials, i.e., the Lennard-Jones potential and the hydrogen-bond potential. Superposing the theoretical curves to the experimental internal pressures and adjusting the increment of the theoretical internal energy to the experimental latent heat, we have resolved the contributions to the latent heat. A large drastic breakdown of the hydrogen bonds at the transition has been expected from this analysis. Most of the decrease in the energy of the hydrogen bonds accompanying the  $\alpha \rightarrow \beta$  transformation should be canceled from the increase in the van der Waals energy.

If the rigid-body thermal vibrations of the two phases are not much different, the problem is the source of the positive latent entropy. It should also be considered that the OH group can occupy plural positions in the configurational space, but this seems unlikely to happen from the neutron scattering. To solve this problem, we have analyzed the energy of hydrogen bonds determined above on the basis of the Lippincott–Schroeder potential model.<sup>18</sup> The distribution of the protons between the covalent bond and the ionic bond has been determined. Over 98% of protons distribute in the covalent well, and the protons in the ionic well are only 1.6% in the  $\alpha$  phase. The breakdown of the covalent bonds induces 10% of the protons in the covalent well to flow into the ionic well during the transition. This redistribution of protons stabilizes the weak hydrogen bonds in  $\beta$  and produces the entropy of the same order of magnitude as the latent entropy of the  $\alpha\beta$  transition.

In the present investigation, we have adopted two different potential functions for the hydrogen bond. One is in terms of the average intermolecular distance (volume) for the analysis of the internal energy of bulk phases, and the other is in terms of the covalent energy and the ionic energy for each hydrogen bond. It is assumed that the functional form of the former is independent of the latter. Strictly speaking, this assumption does not hold true. The potential for the hydrogen bonds in eq 4.2 should be improved by considering the contribution of the intra-hydrogen-bond potential. This improvement, however, increases the number of the parameters that are unable to be determined from the experiments. The present potential function, eq 4.2, has the minimum number of the parameters that are able to be determined from the present experiments.

It is concluded that the  $\alpha\beta$  transition would be induced by the drastic breakdown of the hydrogen bonds accompanied by the redistribution of protons.

**Acknowledgment.** The authors thank K. Sugiyama and J. Katano for their kind help in the DSC measurements.



**Supporting Information Available:** Derivation of the potential energy of the hydrogen-bonded crystal, eq 4.2, and values of parameters (Table 6S) and contributions of the vdW energy and the HB energy (Table 7S). This information is available free of charge via the Internet at <http://pubs.acs.org>.

### References and Notes

- (1) Lautz, H. Z. *Phys. Chem.* **1913**, 84, 611.
- (2) Yoshino, M.; Naoki, M. To be published.
- (3) Robertson, J. M. *Proc. R. Soc. London* **1936**, A157, 79.
- (4) Robertson, J. M.; Ubbelohde, A. R. *Proc. R. Soc. London* **1938**, A167, 122.
- (5) Bacon, G. E.; Curry, N. A. *Proc. R. Soc. London* **1956**, A235, 552.
- (6) Bacon, G. E.; Lisher, E. J. *Acta Crystallogr.* **1980**, B36, 1908.
- (7) Ebisuzaki, Y.; Askari, L. H.; Bryan, A. M.; Nicol, M. F. *J. Chem. Phys.* **1987**, 87, 6659.
- (8) Ban, T.; Suga, H.; Seki, S. *Nihonkagakuzassi* **1971**, 92, 56.
- (9) Robertson, J. M.; Ubbelohde, A. R. *Proc. R. Soc. London* **1938**, A167, 136.
- (10) Suga, H.; Nakatsuka, K.; Shinoda, T.; Seki, S. *Nihonkagakuzassi* **1961**, 82, 29.
- (11) Sabbah, R.; Buluku, E. N. L. E. *Can. J. Chem.* **1991**, 69, 481.
- (12) Deb, S. K.; Rekha, M. A.; Roy, A. P.; Vijayakumar, V.; Meenakshi, S.; Godwal, B. K. *Phys. Rev. B* **1993**, 47, 11491.
- (13) Sharma, S. M.; Vijayakumar, V.; Sikka, S. K.; Chidambaram, R. *Pramana J. Phys.* **1985**, 25, 75.
- (14) Lennard-Jones, J. E.; Devonshire, A. E. *Proc. R. Soc. London, Ser. A* **1937**, 163, 53.
- (15) Lennard-Jones, J. E.; Ingham, A. E. *Proc. R. Soc. London, Ser. A* **1925**, 107, 636.
- (16) Naoki, M.; Ujita, K.; Kashima, S. *J. Phys. Chem.* **1993**, 97, 12356.
- (17) Bondi, A. *Physical Properties of Molecular Crystals, Liquids, and Glasses*; Wiley: New York, 1968.
- (18) Lippincott, E. R.; Schroeder, R. *J. Chem. Phys.* **1955**, 23, 1099.